❒   214

Design of a model for multistage classification of diabetic retinopathy and glaucoma

Rupesh Goverdhan Mundada, Devesh Nawgaje
Department of Electronics and Telecommunication Engineering, Shri Sant Gajanan Maharaj College of Engineering, Shegaon, India

Article Info

ABSTRACT

This study addresses the escalating prevalence of diabetic retinopathy (DR) and glaucoma, major global causes of vision impairment. We propose an innovative iterative Q-learning model that integrates with fuzzy C-means clustering to improve diagnostic accuracy and classification speed. Traditional diagnostic frameworks often struggle with accuracy and delay in disease stage classification, particularly in discerning complex features like exudates and veins. Our model overcomes these challenges by combining fuzzy C means with Q learning, enhancing precision in identifying key retinal components. The core of our approach is a custom-designed 45-layer 2D convolutional neural network (CNN) optimized for nuanced detection of DR and glaucoma stages. Compared to previous approaches, the performance on the IDRID and SMDG-19 datasets and associated samples shows a 10.9% rise in precision, an 8.5% improvement in overall accuracy, an 8.3% enhancement in recall, a 10.4% larger area under the curve (AUC), a 5.9% boost in specificity, and a 2.9% decrease in latency. This methodology has the potential to bring about significant changes in the field of DR and glaucoma diagnosis, leading to prompt medical interventions and possibly decreasing vision loss. The use of sophisticated machine learning techniques in medical imaging establishes a model for future investigations in ophthalmology and other clinical situations.

Corresponding Author:

Rupesh Goverdhan Mundada
Department of Electronics and Telecommunication Engineering
Shri Sant Gajanan Maharaj College of Engineering
Shegaon, Maharashtra, India
Email: rupeshmundada@gmail.com

1.   INTRODUCTION

Diabetic retinopathy (DR) and glaucoma are two of the most common eye diseases that can lead to vision loss. These diseases affect millions of people worldwide. To prevent vision loss, early and accurate detection of these diseases is crucial. Physicians utilize fundus images, a specialized camera, to examine the eyes and identify these diseases. However, reading these images can be hard and takes a lot of delay for clinical scenarios. In the past, scientists have made computer programs to help doctors read these images. But these programs are not always right. They sometimes miss important signs of the disease or take too long to give an answer. This issue is critical as delayed detection of the disease can exacerbate and result in blindness. This paper talks about a new way to use computers to find diabetic retinopathy and glaucoma in fundus images and samples. The new method uses fuzzy C-means and Q-learning. Fuzzy C means a way to group similar things together in an image, like blood vessels or spots that shouldn't be there. Q-learning is a type of learning where

the computer tries different things and learns from its mistakes to get better over time. The new method also uses a special kind of computer program called a 2D convolutional neural network (CNN). The 45 layers of this program enable detailed analysis of the images. It helps to more accurately identify the signs of diabetic retinopathy and glaucoma. We tested the new method on two large sets of eye images, called IDRID and SMDG-19. The results were very good. The new method was better at finding the right stage of the disease compared to the old methods. It was more accurate, faster, and made fewer mistakes.

A study by Hao *et al.* [1] created a hybrid variation-aware network for angle-closure assessment in anterior segment optical coherence tomography (AS-OCT). This showed how computational methods can be used to make diagnostics more accurate. In the same way, Manassakorn *et al.* [2] showed GlauNet, a CNN architecture for optical coherence tomography angiography (OCTA) imaging. This showed how important advanced CNN models are for improving eye diagnostics. Furthermore, Kunumpol *et al.* [3] explored the integration of virtual reality perimetry with artificial intelligence (AI) for glaucoma diagnosis, underscoring the potential of modern technology in enhancing diagnostic accuracy. Advancements in treatment strategies are also evident, such as the research by Silverman *et al.* [4] on high-frequency ultrasound activation for glaucoma treatment, showcasing diverse applications of ultrasound technology in ophthalmology. Studies like Yi *et al.* [5] with MTRA-CNN and Das *et al.* [6] with CA-Net demonstrate significant advancements in glaucoma classification and prediction models, highlighting the effectiveness of specialized neural network architectures in detailed disease classification. Also, Pham *et al.* [7] and Shi *et al.* [8] looked at multimodal deep learning and artifact-tolerant clustering-guided learning models for predicting and analyzing ophthalmic images in glaucoma. This shows how important it is to have strong models that can deal with large datasets. The works [9]–[11] have evidenced advancements in segmentation models, classification techniques, and ophthalmology applications in the realm of DR. These studies collectively represent a dynamic and rapidly evolving field, increasingly leveraging AI, deep learning, and innovative imaging technologies to improve the diagnosis and management of DR and glaucoma [12]–[14], indicating a paradigm shift towards more accurate, efficient, and patient-centric approaches in ophthalmology scenarios. The application of deep learning algorithms and artificial neural network gives better results and provide help to the ophthalmologists [15]–[20].

The research focused on recognizing these diseases individually, and there is little work on expanding modern machine and deep learning models to detect several eye ailments. The main reason is that each eye disease has unique abnormal signals. Additionally, a model designed for one condition may perform poorly for another. However, we addressed this assumption and developed a robust model that can identify and recognize three eye illnesses with high accuracy. Thus, we demonstrated that deep learning algorithms can diagnose different eye problems, like ophthalmologists. In order to tackle these difficulties, this study presents a novel strategy that integrates the advantages of fuzzy C-means clustering, Q-learning, and a specially constructed 45-layer 2D CNN. This combination represents a notable deviation from conventional approaches, providing a more subtle and effective examination of fundus images and samples. The motivation is twofold: to enhance disease detection accuracy and expedite the diagnostic process, facilitating prompt medical intervention.

2. METHODOLOGY

People commonly use fundus scans as a bilateral technique to identify eye issues associated with diabetes. The first stage is detecting and locating the existence of a disease, while the following step requires partitioning the localized areas into separate segments using the Q-learning technique. For the localization step, we utilize the CNN approach. We generate annotations for diseases and subsequently employ CNN training to extract features from photos. We use the FCM clustering methodology for segmentation, widely recognized as a reliable method, particularly for picture segmentation. These features feed into the pooling layer, subsequently serving as input for the group and fully connected layers. We evaluate the model by precisely detecting the affected regions using the test scans and a regression confidence score. Figure 1 illustrates the configuration of the suggested methodology.

The initial stage involves pre-processing the input image and marking the annotations. By comparing the ground-truth bounding box with each image, we must identify the specific affected region to train the model. LabelImg is a software tool that adds annotations to retinal images and manually generates bounding boxes. Figure 2 presents a sample ground-truth photographs for diabetic retinopathy as shown in Figure 2(a) and glaucoma shown in Figure 2(b). XML files store annotations, which include information on the object class and bounding box values (xmin, ymin, xmax, ymax, width, and height). We use the XML file of each

image to create a CSV file, which we then use to generate a train record file for training.

The localization phase is the second phase. CNNs are utilized for DR to analyse images and identify potential areas of concern. The method we employ, which consists of max-pooling and convolutional layers, analyses the entire image and generates the feature map. The pooling layer retrieves fixed-size feature vectors from the feature map of the convolutional layer. Then it is inputted into interconnected layers before diverging into output layers. The multi-class DR object detection model, trained by CNN, can precisely identify multi-class objects within an image. Blood hemorrhages, microaneurysms, soft and hard-exudates, and a backdrop class are employed for the localization of DR.

We trained our skills using glaucoma, OD, OC, and background lessons. CNN successfully detected the OD (optic disc) and OC (optic cup) regions and evaluated the background of the retinal image. The maxpooling and convolutional layers provide the feature map, which is then utilized by the pooling layer to extract feature vectors of a fixed size. After being input into layers, the information then diverges into output layers.
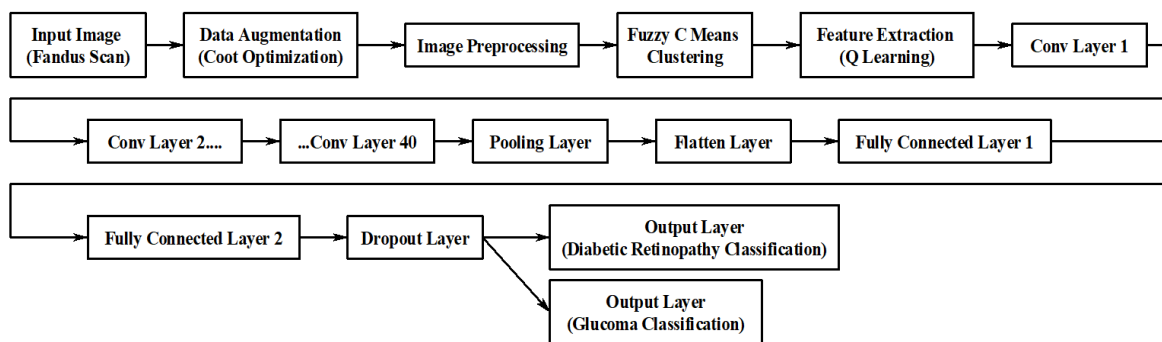

Figure 1. Model architecture for the overall method used for classification of different disease types
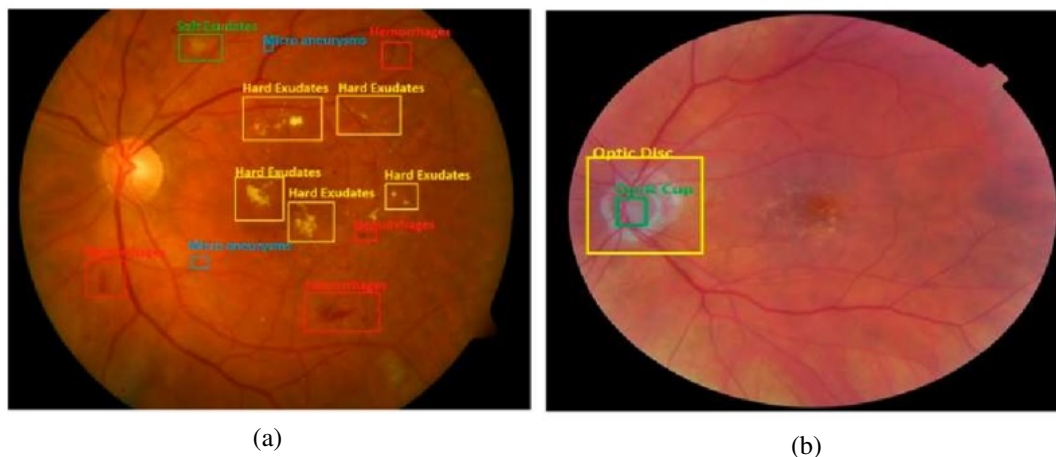

Figure 2. Sample annoted images (a) diabetic retinopathy and (b) glaucoma

The next phase explains mathematical modeling. Figure 1 shows that the suggested model uses a new combination of fuzzy C mean (FCM) clustering and Q learning, which creates a fresh way to separate fundus scans. This process, integral to the model's functioning, begins with the collection of fundus scans, which serve as the input for different use cases. Segmented fundus scans, primed for further analysis and classification of DR and glaucoma levels, are the end goal.

The first step in the model's operation involves applying FCM clustering, an unsupervised method that partitions the input fundus scans into distinct clusters. In (1) estimates the objective function, which defines the FCM algorithm in its essence.

$$Jm(U, V)] = \sum_{i=1}^{n} \sum_{j=1}^{c} u(i,j,m) ||x(i) - v(j)||^2$$ (1)

Where, n is the number of data points (pixels in the fundus scans), c is the number of clusters, u(i,j) is the degree of membership of x(i) in the cluster j, v(j) is the centroid of the cluster, and m is a real number greater than 1 that influences the fuzziness of the clustering process. The optimization of the FCM is conducted through an iterative process, where the update of membership u(i,j) and the cluster centers v(j) are calculated via (2) and (3),

$$u(i,j) = \frac{1}{\sum_{k=1}^{c} \left(\frac{||xi-vk||}{||xi-vj||} \right)^{\frac{2}{m-1}}}$$ (2)

$$vj = \frac{\sum_{i=1}^{n} u(i,j,m) * x(i)}{\sum_{i=1}^{n} u(i,j,m)}$$ (3)

The iterative process continues until the maximum change in u(i,j) between two consecutive iterations is less than a specified threshold, indicating convergence scenarios. Subsequently, the segmented outputs from FCM serve as inputs to the Q learning model process. Q learning, a form of reinforcement learning, adapts its strategy to maximize the reward signals. In the context of image segmentation, the reward signal is designed to favor segmentations that accurately represent the distinct regions within the fundus scans. The reward function R(s,) is formulated based on the degree of segmentation accuracy via (4),

$$R(s, \alpha) = \alpha * Accuracy(s, \alpha) - \beta * Complexity(s, \alpha)$$ (4)

where,   and   are weighting factors that balance the importance of accuracy versus complexity in the segmentation process.   The term accuracy(s,) quantifies the correctness of the segmentation, while, complexity(s,) assesses the computational complexity or simplicity of the segmentation result, ensuring that the model does not overfit or produce overly intricate segmentations.

The list of actions A in this model includes various operations that can be applied to modify the segmentation, such as adjusting the clustering parameters in FCMs, altering the threshold values, and changing the spatial resolution of the segmentation process. Each action aA has the potential to transform the current state of the image segmentation into a new state, ideally improving the segmentation quality levels. The states S in this model are represented by the different possible segmentations of the fundus scans. Each state sS is a distinct configuration of segmented regions within an image, varying based on the parameters and thresholds applied during the segmentation process. The model explores these states through the actions, aiming to discover the state that yields the most accurate segmentation with manageable complexity levels. Based on this, the Q learning model utilizes an iterative Q function, which is defined via (5),

$$Q(s, \alpha) = Q(s, \alpha) + \alpha[R(s, \alpha) + \gamma max\alpha' Q(s', \alpha') - Q(s, \alpha)]$$ (5)

where, s represents the current state (segmented image), a represents an action taken by the model (modifying segmentation parameters), R(s,) is the reward for taking action in state s, is the learning rate, is the discount factor, and s' is the new state after action is taken for different use cases. The Q learning model iteratively updates its Q values based on the reward received from the segmented images, refining the segmentation parameters to optimize the segmentation quality levels. The fusion of FCM and Q learning allows the model to not only segment the fundus images into meaningful clusters but also to refine these clusters iteratively, enhancing the accuracy and precision of the segmentation process. This iterative fusion leads to a more nuanced and sophisticated understanding of the fundus scans, which is pivotal for the accurate diagnosis and classification of ocular diseases.

In the advanced operations of medical image analysis, the proposed model's 45-layer CNN stands as an efficient and unique process, adeptly classifying segmented fundus scans into specific types and stages of

diabetes and glaucoma types. The cornerstone of this model is its deep and complex 45-layer CNN architecture, meticulously designed to capture the subtlest of features in the segmented scans. The first layer of this architecture is a convolutional layer, which performs an operation defined via (6),

$$F(i,j,l) = \sigma\left(b(l) + \sum_{m=0}^{M-1}\sum_{n=0}^{N-1} K(m,n,l) \cdot I\big(i+m, j+n, (l-1)\big)\right) \tag{6}$$

where, F(i,j,l) is the feature map at layer l, is a non-linear activation rectified linear unit (ReLU), b(l) is the bias, K(m,n,l) represents the kernel weights, and I(i+m,j+n,(l-1)) is the input from the previous layers.

Following next 40 convolutional layers, each introducing additional complexity and depth to the feature extraction process, the architecture integrates pooling layers. These layers are designed to reduce the spatial dimensions of the feature maps, enhancing the model's efficiency and its ability to capture more global features. After this, the pooling operation is performed which is defined via (7),

$$P(i,j,l) = max\left(F(k,l,l)|k\epsilon[i,i+K], l\epsilon[j,j+K]\right) \tag{7}$$

where, Pij(l) is the output of the pooling layer, Fkl(l) is the feature map from the previous convolutional layer, and K is the size of the pooling windows. Further into the network, the model employs fully connected layers, which synthesize the learned features into more abstract representations. The operation in a fully connected layer is estimated via (8),

$$A(l) = \sigma\big(W(l) \cdot A(l-1) + b(l)\big) \tag{8}$$

where, A(l) is the activation in layer l, W(l) represents the weights, b(l) is the bias.

The final layers of the CNN, crucial for the classification task, involve softmax functions that convert the activations into probability distributions, indicative of the likelihood of each class and stages. The softmax function for a particular class k is defined via (9),

$$Sk\big((A(L)\big) = \frac{e^{Ak(L)}}{\sum_{j=1}^{c} e^{Ak(L)}} \tag{9}$$

where, Sk(A(L)) is the softmax output for class k, Ak(L) is the activation of the last layer for class k, and C is the total number of classes. This sophisticated CNN architecture is further enhanced by dropout layers interspersed throughout, designed to mitigate the risk of overfitting scenarios. The dropout function for a neuron is represented via (10),

$$F(out) = \{0 \; with \; probability \; p, \; and \; Ai(l), \qquad\qquad with \; probability(1-p)\} \tag{10}$$

where, D(Ai(l)) is the output after dropout, Ai(l) is the activation, and p represents the dropout rate levels. The culmination of this process is the model's ability to classify the segmented fundus scans into specific types of diabetes and glaucoma, followed by a further classification into their respective stages. The model's output layers, employing the softmax function, deliver the final classification, marking the end of a complex journey from image input to detailed medical insights for different scenarios. This model not only showcases the potential of AI in healthcare but also marks a significant stride forward in the battle against these pervasive ocular diseases. Performance of this model was estimated in terms of different metrics, and compared with existing methods in the next section of this article.

3. RESULT AND DISCUSSION

The proposed model is an efficient and pioneering advancement in the field of ophthalmic diagnostics, representing a paradigm shift in the detection and classification of DR and glaucoma from fundus scans. At its core, this model combines a carefully planned 45-layer 2D CNN with the novel techniques of iterative Q learning and FCM clustering. This makes it much better at detecting small changes in the retina that are signs of these conditions. The IQMSDRG model has amazing performance metrics, such as precision and

accuracy rates that are much higher than well-known models like GlauNet, MTRA, and MIMC. This shows how advanced machine learning techniques can change medical imaging for the better. Its ability to accurately classify the stages of DR and glaucoma not only paves the way for timely and targeted medical interventions, but also opens new horizons for research and application in the broader field of medical diagnostics.

We benchmark the IQMSDRG model's outcomes against existing models like GlauNet, MTRA, and MIMC. This comparison is based on metrics like precision, accuracy, recall, specificity, AUC, and processing delays. This experimental setup, with its comprehensive approach to data utilization and rigorous testing protocols, aims to validate the effectiveness of the IQMSDRG model. It underscores the model's potential to significantly enhance the diagnostic accuracy and efficiency in identifying DR and glaucoma, as evidenced by the comparative analysis with existing diagnostic frameworks.

When analyzing the results, a pattern emerges: the proposed IQMSDRG model consistently outperforms the other models in terms of precision across almost all test scan sizes. Figure 3 shown Graphical analysis on various parameters. The precision of the graphical representation is given in Figure 3(b). For instance, at 812 NTS, IQMSDRG exhibits a precision of 92.68%, notably higher than GlauNet (83.45%), MTRA (68.27%), and MIMC (86.83%). This trend continues at 1508 NTS, where IQMSDRG achieves a remarkable precision of 96.28%, surpassing GlauNet's 79.57%, MTRA's 88.43%, and MIMC's 88.74%. The significant precision rates indicate the model's ability to correctly classify a high number of true positive cases, reducing the likelihood of false positives. This is crucial in medical diagnostics, where the accuracy of classification can directly impact patient treatment and management decisions. As the NTS gets higher, IQMSDRG becomes more accurate; for example, it reached 97.18% at 13920 NTS, showing that it can handle large and varied datasets well.

Figure 3(d) presents a comparison of the models' accuracy. Upon analysis, the IQMSDRG model consistently demonstrates superior accuracy in comparison to the other models across a broad range of test scan sizes. For instance, at 812 NTS, the accuracy of IQMSDRG stands at 87.46%, surpassing GlauNet (83.91%), MTRA (84.08%), and MIMC (85.66%). This trend toward superior performance is also evident in other test sizes, such as 1508 NTS, where IQMSDRG achieves 92.80% accuracy, significantly higher than the other models.

Analysing the data, it's evident that the IQMSDRG model exhibits a consistently higher recall rate compared to the other models in most test scenarios. For instance, at 812 NTS, IQMSDRG shows a recall of 93.60%, significantly higher than GlauNet (80.38%), MTRA (76.86%), and MIMC (78.09%). This trend is observable across various NTS, such as 4988 NTS, where IQMSDRG reaches a recall of 93.05%, again outperforming the other models. Furthermore, the consistent performance of IQMSDRG across varying numbers of test scans demonstrates its robustness and adaptability to different clinical settings and patient volumes. After analysing the data, the IQMSDRG model demonstrates consistently higher specificity in comparison to the other models across most NTS values. For instance, at 812 NTS, IQMSDRG achieves a specificity of 88.90%, which is notably higher than GlauNet (73.37%), MTRA (60.65%), and MIMC (76.63%). This trend of higher specificity is evident across various test sizes, such as 4524 NTS, where IQMSDRG records a specificity of 90.98%, outperforming the other models. Higher specificity reduces the likelihood of false positives, which is critical in medical settings to avoid unnecessary patient anxiety and over-treatment or misdiagnosis. Refer Figure 3(c) and 3(e).

Analysing the data, we see that the delay times for the IQMSDRG model are competitive with other models, showcasing its efficiency in processing scans as shown in Figure 3(f). For instance, at 812 NTS, IQMSDRG has a delay of 97.46 ms, which is comparable to MIMC's 94.78 ms and better than GlauNet's 113.69 ms. Across various NTS, IQMSDRG's delay remains within a reasonable range, indicating its consistent performance. For example, at 5568 NTS, IQMSDRG shows a delay of 96.36 ms, demonstrating its ability to maintain efficiency even as the number of scans increases.

Examining the provided data, the IQMSDRG model consistently shows higher AUC values in comparison to the other models across most NTS values. For example, at 812 NTS, IQMSDRG achieves an AUC of 90.03, significantly surpassing GlauNet (78.82), MTRA (75.83), and MIMC (60.14). This trend continues at higher NTSs, such as 6612 NTS, where IQMSDRG has an AUC of 93.78, indicating its superior diagnostic ability. Innovatively integrating iterative Q learning and FCM clustering with a sophisticated 45-layer 2D CNN achieves these results. These technical advancements enable the model to effectively differentiate between the nuanced features of DR and glaucoma, leading to a more accurate classification. Comparison with various implemented method is summarized as per Table 1. Refer Figure 3(a).

Table 1. Comparison of parameters for various methods

Method	Precision (%)	Recall rate (%)	AUC (%)	Specificity (%)	Accuracy (%)	Delay (ms)
GlauNet	83.45	80.38	78.82	73.37	83.91	113.69
MTRA	68.27	76.86	75.83	60.65	84.08	99.96
MIMC	86.83	78.09	60.14	76.63	85.66	94.78
IQMSDRG	92.68	93.6	90.03	88.9	87.46	93.46

(a)

(b)

(c)

(d)

(e)

(f)

Figure 3. Graphical analysis on various parameters: (a) AUC, (b) precision, (c) recall, (d) accuracy, (e) specificity, and (f) delay (ms)

4. CONCLUSION

This study makes a substantial contribution to the field of medical diagnostics, specifically in the identification and classification of DR and glaucoma. The proposed IQMSDRG model has a complex 45-layer 2D CNN, iterative Q learning, and FCM clustering. It performs much better than existing models like GlauNet, MTRA, and MIMC in terms of precision, accuracy, recall, specificity, and AUC. The model demonstrates exceptional competency, as indicated by its impressive precision, which may reach up to 97.18%, and

accuracy, which can peak at 97.27%. These qualities are of utmost importance for ensuring dependable medical diagnoses. The IQMSDRG model has the potential to significantly transform the early identification and precise diagnosis of DR and glaucoma in clinical settings. This technology's high precision and accuracy guarantee dependable detection of disease phases, enabling prompt and appropriate medical interventions. Preventing the advancement of these disorders is crucial, as they are among the primary factors contributing to worldwide vision loss. In conclusion, the IQMSDRG model not only marks a significant advancement in the field of medical imaging and diagnostics for DR and glaucoma but also opens avenues for future innovations in healthcare technology. Its integration with advanced machine learning techniques sets a precedent for tackling complex diagnostic challenges, potentially reshaping the landscape of medical diagnostics and patient care scenarios.

ACKNOWLEDGEMENTS

REFERENCES

[1] J. Hao *et al.*, "Hybrid variation-aware network for angle-closure assessment in AS-OCT," *IEEE Transactions on Medical Imaging*, vol. 41, no. 2, pp. 254–265, 2022, doi: 10.1109/TMI.2021.3110602.

[2] A. Manassakorn *et al.*, "GlauNet: glaucoma diagnosis for OCTA imaging using a new CNN architecture," *IEEE Access*, vol. 10, pp. 95613–95622, 2022, doi: 10.1109/ACCESS.2022.3204029.

[3] P. Kunumpol *et al.*, "GlauCUTU: time until perceived virtual reality perimetry with humphrey field analyzer prediction-based artificial intelligence," *IEEE Access*, vol. 10, pp. 36949–36962, 2022, doi: 10.1109/ACCESS.2022.3163845.

[4] R. H. Silverman, R. Urs, M. Burgess, J. A. Ketterling, and G. Tezel, "High-frequency ultrasound activation of perfluorocarbon nanodroplets for treatment of glaucoma," *IEEE Transactions on Ultrasonics, Ferroelectrics, and Frequency Control*, vol. 69, no. 6, pp. 1910–1916, 2022, doi: 10.1109/TUFFC.2022.3142679.

[5] S. Yi, L. Zhou, L. Ma, and D. Shao, "MTRA-CNN: a multi-scale transfer learning framework for glaucoma classification in retinal fundus images," *IEEE Access*, vol. 11, pp. 142689–142701, 2023, doi: 10.1109/ACCESS.2023.3342910.

[6] D. Das, D. R. Nayak, and R. B. Pachori, "CA-Net: a novel cascaded attention-based network for multistage glaucoma classification using fundus images," *IEEE Transactions on Instrumentation and Measurement*, vol. 72, pp. 1–10, 2023, doi: 10.1109/TIM.2023.3322499.

[7] Q. T. M. Pham, J. C. Han, D. Y. Park, and J. Shin, "Multimodal deep learning model of predicting future visual field for glaucoma patients," *IEEE Access*, vol. 11, pp. 19049–19058, 2023, doi: 10.1109/ACCESS.2023.3248065.

[8] M. Shi *et al.*, "Artifact-tolerant clustering-guided contrastive embedding learning for ophthalmic images in glaucoma," *IEEE Journal of Biomedical and Health Informatics*, vol. 27, no. 9, pp. 4329–4340, 2023, doi: 10.1109/JBHI.2023.3288830.

[9] B. Collar, J. Shah, A. Cox, G. Simon, and P. Irazoqui, "Parylene-C microbore tubing: a simpler shunt for reducing intraocular pressure," *IEEE Transactions on Biomedical Engineering*, vol. 69, no. 3, pp. 1264–1272, 2022, doi: 10.1109/TBME.2021.3123887.

[10] R. Leonardo, J. Goncalves, A. Carreiro, B. Simoes, T. Oliveira, and F. Soares, "Impact of generative modeling for fundus image augmentation with improved and degraded quality in the classification of glaucoma," *IEEE Access*, vol. 10, pp. 111636–111649, 2022, doi: 10.1109/ACCESS.2022.3215126.

[11] K. Aurangzeb, R. S. Alharthi, S. I. Haider, and M. Alhussein, "An efficient and light weight deep learning model for accurate retinal vessels segmentation," *IEEE Access*, vol. 11, pp. 23107–23118, 2023, doi: 10.1109/ACCESS.2022.3217782.

[12] T. Fedullo *et al.*, "Assessment of a vision-based technique for an automatic van herick measurement system," *IEEE Transactions on Instrumentation and Measurement*, vol. 71, pp. 1–11, 2022, doi: 10.1109/TIM.2022.3196323.

[13] X. Hu *et al.*, "GLIM-Net: chronic glaucoma forecast transformer for irregularly sampled sequential fundus images," *IEEE Transactions on Medical Imaging*, vol. 42, no. 6, pp. 1875–1884, 2023, doi: 10.1109/TMI.2023.3243692.

[14] S. Krishnan, J. Amudha, and S. Tejwani, "Gaze exploration index (GE i)-explainable detection model for glaucoma," *IEEE Access*, vol. 10, pp. 74334–74350, 2022, doi: 10.1109/ACCESS.2022.3188987.

[15] Y. Meng *et al.*, "Dual consistency enabled weakly and semi-supervised optic disc and cup segmentation with dual adaptive graph convolutional networks," *IEEE Transactions on Medical Imaging*, vol. 42, no. 2, pp. 416–429, 2023, doi: 10.1109/TMI.2022.3203318.

[16] D. Seo *et al.*, "An RC Delay-based pressure-sensing system with energy-efficient bit-level oversampling techniques for implantable IOP monitoring systems," *IEEE Journal of Solid-State Circuits*, vol. 58, no. 10, pp. 2745–2756, 2023, doi: 10.1109/JSSC.2023.3286796.

[17] R. Li *et al.*, "Simultaneous assessment of the whole eye biomechanics using ultrasonic elastography," *IEEE Transactions on Biomedical Engineering*, vol. 70, no. 4, pp. 1310–1317, Apr. 2023, doi: 10.1109/TBME.2022.3215498.

[18] B. N. Jagadesh, M. G. Karthik, D. Siri, S. K. K. Shareef, S. V. Mantena, and R. Vatambeti, "Segmentation using the IC2T model and classification of diabetic retinopathy using the rock hyrax swarm-based coordination attention mechanism," *IEEE Access*, vol. 11, pp. 124441–124458, 2023, doi: 10.1109/ACCESS.2023.3330436.

[19] W. Nazih, A. O. Aseeri, O. Y. Atallah, and S. El-Sappagh, "Vision Transformer model for predicting the severity of diabetic retinopathy in fundus photography-based retina images," *IEEE Access*, vol. 11, pp. 117546–117561, 2023, doi: 10.1109/ACCESS.2023.3326528.

[20] R. G. Mundada and D. D. Nawgaje, "U-Net-based gannet sine cosine algorithm enabled lesion segmentation and deep CNN for diabetic retinopathy classification," *Computer Methods in Biomechanics and Biomedical Engineering: Imaging and Visualization*, vol. 11, no. 6, pp. 2400–2417, 2023, doi: 10.1080/21681163.2023.2236233.

BIOGRAPHIES OF AUTHORS

Rupesh Goverdhan Mundada 🆔 � 🆂🅲 ↻ received his bachelor's and Master's degree from Shri Sant Gajanan Maharaj College of Engineering, Shegaon in 2010 and 2013 respectively. He is currently a research Scholar at Electronics and Telecommunication Engineering Department. His main research interests focus on medical image processing. He can be contacted at email: rupeshmundada@gmail.com.

Dr. Devesh Nawgaje 🆔 � 🆂🅲 ↻ received his B.E. and M.E. and Ph.D. in Electronics and Telecommunication Engineering from Sant Gadge Baba Amravati University, Maharashtra, India. He is currently working as an Associate Professor with the Department of Electronics and Telecommunication Engineering at Shri Sant Gajanan Maharaj College Engineering, Shegaon. His main research interests focus on bio-inspired computing, artificial intelligence, data mining, and text mining. He can be contacted at email: dnawgaje@gmail.com.